

# Vibrational Equilibration in Absorption Difference Spectra of Chlorophyll *a*

Walter S. Struve

Ames Laboratory-USDOE and Department of Chemistry, Iowa State University, Ames, Iowa 50011 USA

**ABSTRACT** We describe Franck-Condon simulations of vibrational cooling effects on absorption difference spectra in chlorophyll *a* (Chl *a*). The relative contributions of vibrational equilibration in the electronic ground and excited states depend on the pump and probe wavelengths. For Franck-Condon-active vibrational modes exhibiting small Huang-Rhys factors ( $S < 0.1$ , characteristic in Chl *a* pigments), vibrational thermalization causes essentially no spectral changes when the origin band is excited. Significant spectral evolution does occur for  $S < 0.1$  when the 0–1 and 1–0 (hot) vibronic bands are excited. However, vibrational equilibration in these cases causes no spectral shifting in the empirical photobleaching/stimulated emission band maximum. This result bears on the interpretation of time-resolved absorption difference spectra of Chl *a*-containing antennae such as the Chl *a/b* light-harvesting peripheral antenna of photosystem II.

## INTRODUCTION

The use of femtosecond lasers to study primary processes in photosynthetic antennae has raised questions about the extent to which subpicosecond processes other than electronic energy transfers may influence their absorption difference spectra. While analyzing the absorption difference spectroscopy of bacteriochlorophyll (BChl) *a* monomers excited in the  $Q_x$  band in polar solvents, Becker et al. (1991) found that their  $Q_y$  photobleaching/stimulated emission (PB/SE) bands exhibited complicated red-shifting kinetics with rate constants ranging from  $\sim 1$  ps to several tens of picoseconds. Because the  $Q_y$  states in these experiments were prepared by internal conversion from the higher-lying  $Q_x$  state, the nascent  $Q_y$  states were generated with some  $4000\text{ cm}^{-1}$  of excess vibrational energy. The PB/SE Stokes shifting could thus arise in principle from a combination of vibrational cooling and dielectric relaxation in the polar solvents. The two mechanisms' relative contributions to the spectral evolution were not separated. Savikhin and Struve (1994a) studied the femtosecond pump-probe spectroscopy of BChl *a* monomers excited directly in the  $Q_y$  band in 1-propanol. By preparing the  $Q_y$  state with vibrational energies ranging from 0 to  $170\text{ cm}^{-1}$  (and by exciting vibrational hot bands situated up to  $\sim 500\text{ cm}^{-1}$  to the red of the  $Q_y$  origin wavelength), they attempted to simulate the range of excess vibrational energies that would be encountered in pump-probe studies of BChl *a*-containing antennae. The subpicosecond spectral evolution found in their one- and two-color experiments could not be explained in terms of dielectric relaxation alone, and it was concluded that vibrational cooling must influence the absorption difference kinetics of BChl *a* monomers.

Two important questions were not addressed by these experiments. It was unclear to what extent the absorption difference experiments detected vibrational cooling in the  $Q_y$  state (through spectral evolution in SE), as opposed to vibrational equilibration in the electronic ground state (through spectral evolution in PB). Second, the effects of vibrational equilibration on absorption difference spectral evolution were not analyzed. It is frequently assumed that cooling of a vibrationally hot state will produce a Stokes shift in the PB/SE spectrum, whereas uphill thermalization in an electronic state prepared with a larger than Boltzmann population in the vibrationless level will cause an anti-Stokes shift. In this study, we show that this assumption is only true for vibrational equilibration in modes with sufficiently large Franck-Condon factors. The spectrally active modes for the  $Q_y$  transitions of chlorophyll *a* (Chl *a*) (and presumably BChl *a*) exhibit small Franck-Condon factors, and the absorption difference changes accompanying vibrational equilibration in these photosynthetic pigments prove to be more subtle. Because an awareness of signatures for vibrational equilibration is potentially important for interpreting the absorption difference spectroscopy of photosynthetic systems, we have simulated its effects in model systems whose vibrational frequencies and Franck-Condon factors resemble those of Chl *a* pigments.

## THEORY

We consider an electronic transition with a single spectrally active vibrational mode of frequency  $\omega_0$ . Before excitation by a laser pulse, the thermal equilibrium populations  $N_v''(0)$  for this mode's vibrational levels in the electronic ground state are

$$N_v''(0) = \frac{N \exp(-v\beta\hbar\omega_0)}{\sum_{v=0}^{\infty} \exp(-v\beta\hbar\omega_0)} \quad (1)$$

$$= N \exp(-v\beta\hbar\omega_0)(1 - \exp(-\beta\hbar\omega_0))$$

Received for publication 16 March 1995 and in final form 5 September 1995.

Address reprint requests to Dr. Walter S. Struve, Department of Chemistry, Iowa State University, Gilman Hall, Ames, IA 50011-3111. Tel.: 515-294-4276; Fax: 515-294-1699; E-mail: wstruve@ameslab.gov.

© 1995 by the Biophysical Society

0006-3495/95/12/2739/06 \$2.00

where  $N$  is the total population in all vibrational states and  $\beta = 1/kT$ . We assume for simplicity that no vibrational frequency shift accompanies the electronic transition. When the 0–0 origin band is excited,  $dN$  molecules are removed from the  $\nu = 0$  level in the electronic ground state and  $dN$  molecules are created with  $\nu = 0$  in the excited state. Because the 1–1 hot band spectrally overlaps the 0–0 transition,  $\exp(-\hbar\omega_0/kT)(F_{11}/F_{00})dN$  molecules will simultaneously be removed from  $\nu = 1$  in the electronic ground state and the same number of molecules will be prepared with  $\nu = 1$  in the electronic excited state. Here  $F_{ij}$  is the Franck-Condon factor (DeVault, 1981) between vibrational states  $i$  and  $j$ . In what follows, we will use  $x$  to abbreviate the Boltzmann factor  $\exp(-\hbar\omega_0/kT)$ . Because the hot bands 2–2, 3–3, etc. will also become excited, this process generates the prompt (nonequilibrium) vibrational populations

$$\begin{aligned} N'_0 &= dN \\ N'_1 &= x(F_{11}/F_{00})dN \\ N'_2 &= x^2(F_{22}/F_{00})dN \\ N'_3 &= x^3(F_{33}/F_{00})dN \\ &\dots \end{aligned} \quad (2)$$

in the electronic excited state and the prompt populations

$$\begin{aligned} N''_0 &= N(1-x) - dN \\ N''_1 &= Nx(1-x) - x(F_{11}/F_{00})dN \\ N''_2 &= Nx^2(1-x) - x^2(F_{22}/F_{00})dN \\ N''_3 &= Nx^3(1-x) - x^3(F_{33}/F_{00})dN \\ &\dots \end{aligned} \quad (3)$$

in the electronic ground state. During vibrational equilibration (assuming no electronic state changes occur via radiative or nonradiative processes), these populations will evolve into

$$\begin{aligned} N'_\nu &= Qx^\nu(1-x)dN \\ N''_\nu &= (N - QdN)x^\nu(1-x) \end{aligned} \quad (4)$$

where

$$Q = 1 + xF_{11}/F_{00} + x^2F_{22}/F_{00} + x^3F_{33}/F_{00} + \dots$$

Equations 3 and 4 show that the prompt populations in the electronically excited state will become redistributed among the other vibrational levels, and the population deficits created by the laser pulse in the electronic ground state will become thermalized. Vibrational equilibration thus occurs simultaneously in both electronic states. At finite temperatures, vibrational redistribution will therefore occur even when the origin band of an electronic transition is directly excited; it is unnecessary to prepare an electronic excited state with excess vibrational energy. Equations 2–4 are easily generalized to excitation of vibrational bands other

than 0–0 and its overlapping hot bands. Equation 4 ensures that the final state distributions conform to a Boltzmann equilibrium.

The spectral effects of vibrational equilibration in pump-probe experiments may be expressed using the functions  $P_\nu(\omega)$  and  $S_\nu(\omega)$ .  $P_\nu(\omega)$  is the photobleaching spectrum for vibrational level  $\nu$  in the electronic ground state;  $S_\nu(\omega)$  is the stimulated emission spectrum of level  $\nu$  in the excited state. These functions, which are defined to be positive-definite, contain the vibrational overlap (Franck-Condon) contributions to the spectra. They omit the factors arising from the electronic transition moment: for rigid pigments, the integrated Einstein coefficients for absorption (hence PB) and SE are equal, so that the PB and SE spectra exhibit the same electronic factor. We do not consider contributions from excited state absorption, because the vibrational structure in the excited state absorption transition(s) is unknown and because the absorption difference spectrum of Chl *a* and BChl *a* monomers is strongly dominated by PB and SE at wavelengths near the 0–0 absorption band maximum. The prompt PB/SE spectrum after exciting the origin (0–0) band will be

$$\begin{aligned} -\Delta A_0(\omega) &= dN \left[ P_0(\omega) + S_0(\omega) + x(F_{11}/F_{00})(P_1(\omega) + S_1(\omega)) \right. \\ &\quad \left. + x^2(F_{22}/F_{00})(P_2(\omega) + S_2(\omega)) + \dots \right] \end{aligned} \quad (5)$$

whereas the equilibrated PB/SE spectrum will be

$$\begin{aligned} -\Delta A_\infty(\omega) &= QdN \left[ (1-x)P_0(\omega) + x(1-x)P_1(\omega) + x^2(1-x)P_2(\omega) + \dots \right. \\ &\quad \left. + (1-x)S_0(\omega) + x(1-x)S_1(\omega) + x^2(1-x)S_2(\omega) + \dots \right] \end{aligned} \quad (6)$$

in accordance with Eqs. 1–4. Using  $l(\omega)$  to represent the vibrational band shape, the photobleaching spectra of the first few ground-state vibrational levels will be

$$\begin{aligned} P_0(\omega) &= F_{00}l(\omega) + F_{01}l(\omega - \omega_0) + F_{02}l(\omega - 2\omega_0) + \dots \\ P_1(\omega) &= F_{10}l(\omega + \omega_0) + F_{11}l(\omega) + F_{12}l(\omega - \omega_0) + \dots \\ P_2(\omega) &= F_{20}l(\omega + 2\omega_0) + F_{21}l(\omega + \omega_0) + F_{22}l(\omega) + \dots \end{aligned} \quad (7)$$

whereas the stimulated emission spectra of the first few excited state levels will be

$$\begin{aligned} S_0(\omega) &= F_{00}l(\omega) + F_{01}l(\omega + \omega_0) + F_{02}l(\omega + 2\omega_0) + \dots \\ S_1(\omega) &= F_{10}l(\omega - \omega_0) + F_{11}l(\omega) + F_{12}l(\omega + \omega_0) + \dots \\ S_2(\omega) &= F_{20}l(\omega - 2\omega_0) + F_{21}l(\omega - \omega_0) + F_{22}l(\omega) + \dots \end{aligned} \quad (8)$$

If the vibrational states in the electronic ground and excited states are eigenfunctions of Hamiltonians for displaced harmonic oscillators of identical frequency  $\omega$ ,

$$\hat{H}_g = -\frac{\hbar^2}{2\mu} \frac{\partial^2}{\partial Q^2} + \frac{1}{2} \mu \omega^2 Q^2 \quad (9)$$

$$\hat{H}_e = -\frac{\hbar^2}{2\mu} \frac{\partial^2}{\partial Q^2} + \frac{1}{2} \mu \omega^2 (Q - \Delta)^2$$

the Franck-Condon factors may be calculated (Manneback, 1951) using the dimensionless Huang-Rhys parameter  $S = \mu\omega\Delta^2/2\hbar$ ,

$$F_{v,v+p} = v!(v+p)!S^p e^{-S} \left[ \sum_{i=0}^v \frac{(-S)^i}{i!(v-i)!(p+i)!} \right]^2 \quad (10)$$

The most intense member  $F_{0v}$  in the sequence of Franck-Condon factors  $F_{00}, F_{01}, F_{02}, \dots$ , occurs for  $v \approx S$ . For Huang-Rhys factors significantly less than 1 (corresponding to small displacements  $\Delta$  between equilibrium geometries), most of the Franck-Condon intensity in this sequence is concentrated in the 0–0 transition.

## MODEL CALCULATIONS

Vibrational cooling effects in absorption difference spectra are sensitive to the Huang-Rhys parameter  $S$ , the vibrational frequency  $\omega_0$ , and the extent of inhomogeneous broadening. For realism, the inhomogeneous broadening is simulated using Gaussian profiles  $I(\omega)$  with  $500 \text{ cm}^{-1}$  fwhm, which is typical for absorption spectra of Chl *a* and BChl *a* pigments in polar solvents (Houssier and Sauer, 1970; Becker et al., 1991). The simulations in Fig. 1 illustrate the contributions of ground- and excited-state vibrational equilibration to spectral evolution in PB and SE, respectively. For clarity of presentation, we use a relatively large Huang-Rhys parameter ( $S = 1$ ). The vibrational mode frequency  $\omega_0$  is  $500 \text{ cm}^{-1}$ , the wavelength of the origin transition is 660 nm, and

the temperature is 300 K. Excitation of the 0–0 origin band yields the prompt PB and SE spectra shown in Fig. 1 *a*. The prompt PB spectrum is dominated by 0–0 and 0–1 bands at 660 and 638 nm, respectively, owing to their large Franck-Condon factors ( $F_{00} = F_{01} = 0.368$  for  $S = 1.0$ ). The prompt SE spectrum (which is the mirror image of the prompt PB spectrum in frequency space) is similarly dominated by 0–0 and 0–1 transitions at 660 and 682 nm, respectively. These prompt spectra (and the equilibrated spectra simulated below) do not take solvent dielectric relaxation into account, because our calculations are limited to spectral effects of vibrational equilibration. The sum of the prompt PB and SE spectra (Fig. 1 *b*) is a symmetric PB/SE spectrum centered at 660 nm. The vibrationally equilibrated PB/SE spectrum (superimposed on the prompt spectrum in Fig. 1 *b*) resembles the prompt spectrum but is readily distinguishable from it; such spectral equilibration would easily be observed under signal/noise ratios available in current pump-probe techniques (Hess et al., 1993; Savikhin et al., 1994). In Fig. 1 *c*, we show the prompt PB and SE spectra for the case where the 0–1 band and its overlapping 1–2, 2–3, etc., hot bands are excited at 638 nm. Whereas the prompt PB spectrum is similar to the one in Fig. 1 *a*, the prompt SE spectrum is dominated by 1–0, 1–2, and 1–3 transitions at 638, 682, and 707 nm. (The low SE signal at 660 nm occurs because the Franck-Condon factor  $F_{11}$  vanishes for  $S = 1$ ; cf. Eq. 10.) The combined prompt and equilibrated spectra for 0–1 band excitation, shown in Fig. 1 *d*, exhibit a large red shift in the empirical PB/SE band maximum (from 638 to 660 nm). Most of the spectral evolution in this case clearly stems from dynamic changes in the SE (rather than PB) spectrum, because of vibrational cooling in the excited electronic state. Fig. 1, *e* and *f*, shows the corresponding spectra for excitation of the 1–0 hot band at 682 nm. Here the composite PB/SE band maximum exhibits a dynamic blue shift (from 682 to 660 nm); most of this evolution arises from the effect on the PB spectrum of vibrational cooling in the electronic ground state. The relative contributions of ground- and excited-state vibrational equilibration thus depend on the excitation wavelength. We emphasize in passing that these results for  $S = 1$  present no new physical insights, inasmuch as the spectral effects of vibrational cooling in vibrational modes with significant Huang-Rhys factors are already widely appreciated. We are primarily concerned here with the case in which  $S$  becomes small, as in Chl *a* pigments.

In Fig. 2, we show prompt and equilibrated PB/SE spectra for smaller Huang-Rhys parameters,  $S = 0.5$  and  $0.1$ . All other parameters are the same as in Fig. 1. The absorption difference spectra for  $S = 0.5$  in Fig. 2, *a–c*, bear a family resemblance to those for  $S = 1$ . The spectral evolution after excitation of the origin at 660 nm, though diminished relative to that for  $S = 1$ , is still observable. Excitation of the 0–1 or 1–0 transition at 638 or 682 nm promptly yields a broad, asymmetric PB/SE spectrum, which then sharpens into an equilibrated spectrum centered at 660 nm. The respective prompt PB/SE spectra exhibit shoulders to the

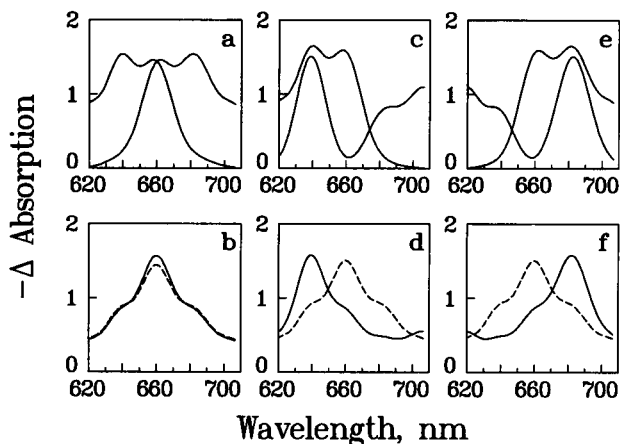


FIGURE 1 Simulated absorption difference spectra for an electronic transition (origin at 660 nm) coupled to a vibrational mode with frequency  $\omega_0 = 500 \text{ cm}^{-1}$  and Huang-Rhys factor  $S = 1.0$ . The vibrational band profile  $I(\omega)$  is Gaussian with  $500 \text{ cm}^{-1}$  fwhm. (a) Prompt photobleaching and stimulated emission spectra for 0–0 excitation at 660 nm, left- and right-hand curves, respectively; (b) total prompt (solid line) and equilibrated (dashed line) absorption difference spectra for 0–0 excitation; (c) prompt photobleaching and stimulated emission spectra for 0–1 excitation at 638 nm; (d) total prompt (solid line) and equilibrated (dashed line) absorption difference spectra for 0–1 excitation; (e) prompt photobleaching and stimulated emission spectra for 1–0 hot band excitation at 682 nm; (f) total prompt (solid line) and equilibrated (dashed line) absorption difference spectra for 1–0 excitation.

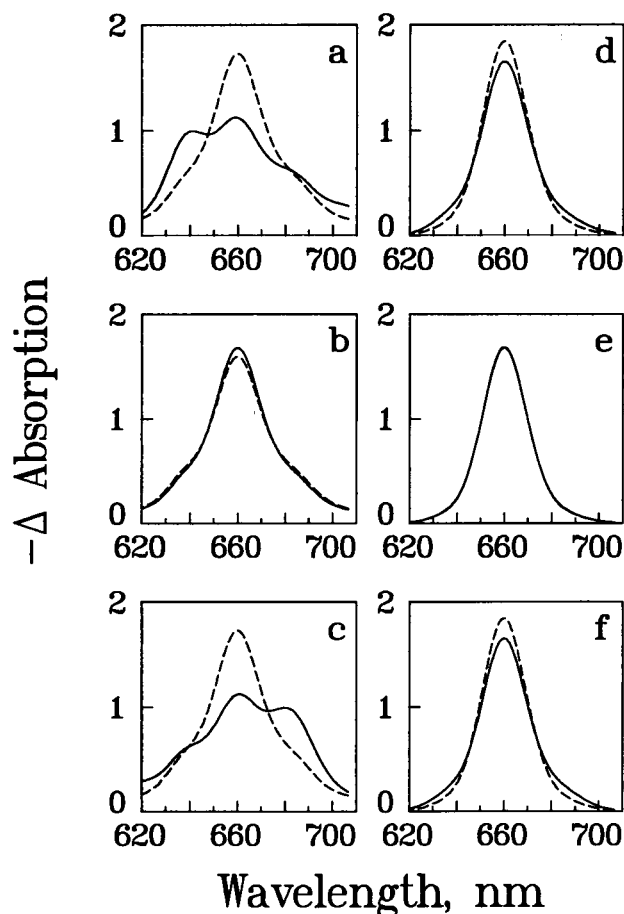


FIGURE 2 Total prompt (solid line) and equilibrated (dashed line) absorption difference spectra for the same electronic transition as in Fig. 1, except that the Huang-Rhys factors are  $S = 0.5$  (left column) and  $S = 0.1$  (right column). The pumped vibrational bands are 0–1 excited at 638 nm (top), 0–0 excited at 660 nm (middle), and 1–0 excited at 682 nm (bottom).

blue and to the red of the 660 nm origin wavelength. These shoulders are vestiges of the well-defined PB/SE maxima that appear in the prompt spectra for  $S = 1$  (Fig. 1). The spectral metamorphoses due to vibrational equilibration for  $S = 0.5$  are thus not well described in terms of red or blue shifting in the position of the PB/SE band maximum. For  $S = 0.1$ , vibrational equilibration upon excitation of the origin band causes almost no discernible spectral evolution (Fig. 2 *e*). Exciting the 0–1 or 1–0 bands (Fig. 2, *d* and *f*) generates prompt PB/SE spectra that are nearly symmetric about the origin wavelength (in contrast to the cases where  $S = 1$  and 0.5). These prompt spectra evolve into an equilibrated spectrum with diminished intensity in the wings and increased intensity near 660 nm. For such small Huang-Rhys parameters, vibrational equilibration subtly influences the shape of the PB/SE spectrum, without shifting the position of the PB/SE band maximum. However, the fractional absorption difference changes under 0–1 or 1–0 excitation are easily detectable at many wavelengths for  $S = 0.1$ , particularly in the wings of the difference spectra.

## CHLOROPHYLL

The steady-state  $Q_y$  absorption spectra of Chl *a* and BChl *a* monomers are strongly dominated by intense origin bands, located in the neighborhood of 660 and 770 nm, respectively, in polar solvents. A broad, weak shoulder on the blue side of this band, frequently termed a “0–1” vibronic feature (Gouterman, 1978), is actually a sequence of overlapping 0–1 bands in vibrational modes carrying small Huang-Rhys factors ( $S \leq 0.05$  in the case of Chl *a*; Gillie et al., 1989). Hence, the regime for Franck-Condon effects on spectral evolution resembles the one shown for  $S = 0.1$  in Fig. 2. Gillie et al. (1989) determined the frequencies and Huang-Rhys factors for 41 Chl *a* intramolecular vibrational modes in a spectral hole-burning study of the Chl *a* core antenna in photosystem I particles from spinach. The frequencies of these intramolecular modes range from 262 to 1524  $\text{cm}^{-1}$ . Among the modes with frequency  $< 750 \text{ cm}^{-1}$ , the most active ones occur at 746  $\text{cm}^{-1}$  ( $S = 0.044$ ), 521  $\text{cm}^{-1}$  ( $S = 0.017$ ), 469  $\text{cm}^{-1}$  ( $S = 0.019$ ), and 390  $\text{cm}^{-1}$  ( $S = 0.015$ ). Fig. 3 shows simulations of the absorption

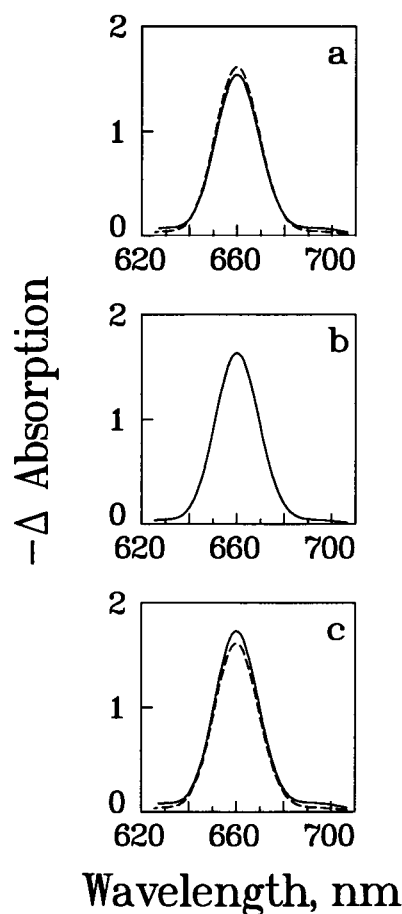


FIGURE 3 Total prompt (solid line) and equilibrated (dashed line) absorption difference spectra for a 660 nm electronic transition coupled to a 746  $\text{cm}^{-1}$  mode with  $S = 0.044$ . The vibrational band profile  $I(\omega)$  is Gaussian with 500  $\text{cm}^{-1}$  fwhm. The pumped vibrational transitions are (from top) 0–1, 0–0, and 1–0, excited at 629, 660, and 694 nm, respectively.

difference spectra for a 660 nm electronic transition coupled to 746  $\text{cm}^{-1}$  mode with  $S = 0.044$ , excited in its 0–0, 0–1, and 1–0 bands. Whereas no spectral equilibration is observable in the first case, thermalization will produce large fractional absorption difference changes ( $\sim 50\%$ ) at the pump wavelength when the 0–1 (629 nm) or 1–0 (694 nm) bands are excited. The simulated spectral changes in the 469  $\text{cm}^{-1}$  mode are considerably smaller (Fig. 4), primarily because of the smaller Huang-Rhys factor. However, Fig. 4 also shows that using a narrower vibrational profile (i.e., using a 250  $\text{cm}^{-1}$  instead of 500  $\text{cm}^{-1}$  fwhm Gaussian for  $I(\omega)$ ) accentuates the fractional changes in the absorption difference signals at the pump wavelengths for 0–1 and 1–0 excitation. Hence, even vibrational cooling in this mode with  $S = 0.019$  can influence the empirical ultrafast pump-probe kinetics in Chl *a*-protein complexes, where inhomogeneous broadening of the  $Q_y$  absorption is often appreciably smaller (Gillie et al., 1989) than for Chl *a* monomers in solution.

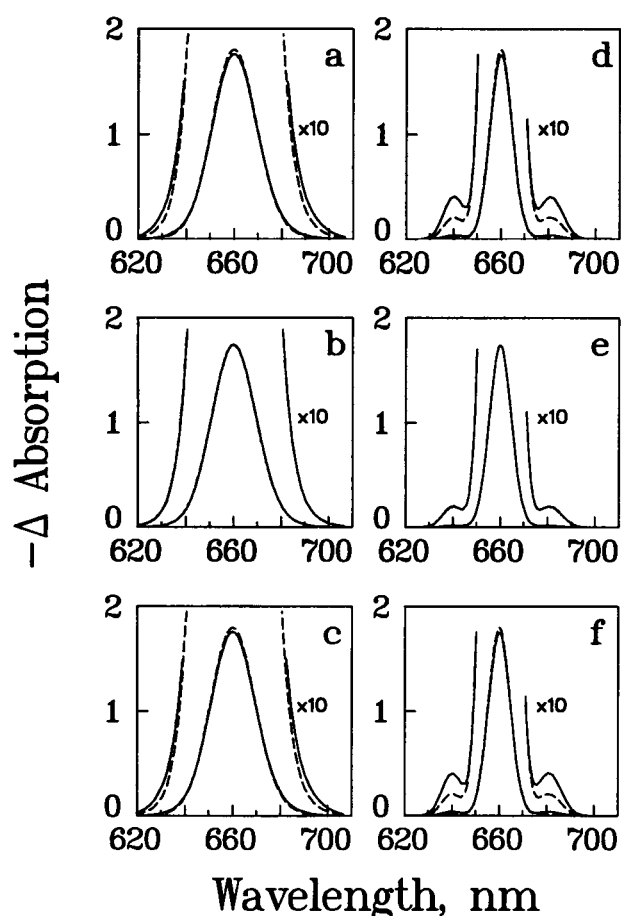


FIGURE 4 Total prompt (solid line) and equilibrated (dashed line) absorption difference spectra for a 660 nm electronic transition coupled to a 469  $\text{cm}^{-1}$  mode with  $S = 0.019$ . The vibrational band profiles are Gaussians with inhomogeneous broadening of 500  $\text{cm}^{-1}$  fwhm (left column) and 250  $\text{cm}^{-1}$  fwhm (right column). The pumped vibrational transitions are (from top) 0–1, 0–0, and 1–0, excited at 640, 660, and 681 nm, respectively.

Some of the spectrally active vibrational modes at still higher frequencies occur at 1259, 1364, and 1524  $\text{cm}^{-1}$ , with  $S = 0.041$ , 0.032, and 0.032, respectively (Gillie et al., 1989). In pump-probe experiments using  $\sim 100$  fs transform-limited laser pulses, the output bandwidth will typically be on the order of 150  $\text{cm}^{-1}$ . Realistic simulations of vibrational cooling effects on absorption difference spectra thus require spectral averaging over the excitation bandwidth as well as inhomogeneous broadening. The qualitative conclusions of this section are unaffected, as long as the laser bandwidth and inhomogeneous broadening are smaller than the vibrational mode frequencies of interest. The inhomogeneous broadening in the Chl *a* spectrum of the Chl *a/b* light-harvesting antenna of photosystem II (LHC-II) is 100–120  $\text{cm}^{-1}$  (Kwa et al., 1992; Krawczyk et al., 1993), which is considerably lower than the Chl *a* mode frequencies considered above. On the other hand, the inhomogeneous broadening for BChl *a* monomers in polar solvents is  $\sim 500$   $\text{cm}^{-1}$  (Becker et al., 1991); spectral averaging will considerably influence the empirical vibrational cooling in this case.

Several time-resolved experiments have focused on the kinetics of Chl *b*  $\rightarrow$  Chl *a* energy transfers after excitation of the higher-energy Chl *b* pigments in LHC-II (Gillbro et al., 1985; Eads et al., 1989; Kwa et al., 1992; Bittner et al., 1994). Upon excitation of the Chl *b* antenna of LHC-II, the prompt PB/SE band maximum near 650 nm is rapidly superseded by a PB/SE spectrum that peaks at wavelengths of  $>675$  nm (Kwa et al., 1992). Because the  $Q_y$  energy of Chl *b* pigments absorbing at  $\sim 650$  nm lies some 650  $\text{cm}^{-1}$  above that of the lowest-energy Chl *a* pigments absorbing near 680 nm, the question arises whether some of this spectral shifting in the PB/SE band maximum stems from cooling of vibrationally hot Chl *a* pigments formed via energy transfers from Chl *b*. The simulations shown in Figs. 3–4 clearly show that vibrational cooling cannot be responsible for this spectral shifting. However, it can materially contribute to the pump-probe kinetics observed under fixed probe wavelengths in one- and two-color experiments (Gillbro et al., 1985; Kwa et al., 1992; Bittner et al., 1994).

To our knowledge, the Huang-Rhys parameters for the vibrational modes active in the  $Q_y$  spectrum of BChl *a* have not been determined. Although the  $Q_y$  absorption spectrum of BChl *a* is strongly dominated by the origin transition as in Chl *a* (suggesting that the Huang-Rhys factors are small in BChl *a* as in Chl *a*), the absorption and steady-state fluorescence spectra of BChl *a* do not approximately obey the Stepanov relation, unlike those of Chl *a* (Becker et al., 1991; P. Laible and T. G. Owens, private communication). Hence, comparisons of BChl *a* pump-probe experiments (Hess et al., 1993; Chachisvilis et al., 1994; Savikhin et al., 1994; Savikhin and Struve, 1994a,b) with simulations of vibrational cooling effects await clarification of the electronic-vibrational couplings in this pigment. If these prove to be similar in BChl *a* and Chl *a*, vibrational cooling cannot contribute to the time-dependent shifts in

the PB/SE maxima that have been characterized for BChl *a* in polar solvents (Becker et al., 1991).

## SUMMARY

The following conclusions may be drawn from our Franck-Condon simulations of the effects of vibrational equilibration on time-resolved PB/SE spectra:

1. The relative contributions of ground- and excited-state vibrational equilibration to the absorption difference kinetics in a pump-probe experiment depend on the pump and probe wavelengths.

2. For sufficiently large Huang-Rhys factors ( $S \geq 0.5$ ), marked spectral evolution can occur even when the origin band is excited (cf. Figs. 1 *b* and 2 *b*). For smaller Huang-Rhys factors (as are common for Franck-Condon active modes in Chl *a* pigments), vibrational thermalization does not cause significant spectral changes after exciting the origin band.

3. For the Huang-Rhys factors that are prevalent in Chl *a* ( $S < 0.1$ ), vibrational equilibration effects changes in the shape of the empirical PB/SE spectrum without causing spectral shifts in the PB/SE band maximum (cf. Figs. 2, *d-f*, 3, and 4). It is therefore likely that the red shifting observed in the PB/SE band maximum for BChl *a* monomers in polar solvents (Becker et al., 1991) arises from solvent dielectric relaxation. For similar reasons, spectral shifting of PB/SE band maxima in Chl *a* pigment-protein complexes cannot stem from vibrational cooling (e.g., of vibrationally hot excitation acceptor pigments subsequent to electronic energy transfers).

*Note added in proof:* Intramolecular vibrational redistribution (IVR) is not considered in these calculations. Knowledge of vibrational mode couplings will enable prediction of IVR effects on spectral evolution.

The Ames Laboratory is operated for the U.S. Department of Energy by Iowa State University under contract no. W-7405-Eng-82. This work was supported by the Division of Chemical Sciences, Office of Basic Energy Sciences.

## REFERENCES

- Becker, M., V. Nagarajan, and W. W. Parson. 1991. Properties of the excited-singlet states of bacteriochlorophyll *a* and bacteriopheophytin *a* in polar solvents. *J. Am. Chem. Soc.* 113:6840–6848.
- Bittner, T., K.-D. Irrgang, G. Renger, and M. R. Wasielewski. 1994. Ultrafast excitation energy transfer and exciton-exciton annihilation processes in isolated light harvesting complexes of photosystem II (LHC II) from spinach. *J. Phys. Chem.* 98:11821–11826.
- Chachisvilis, M., T. Pullerits, M. R. Jones, C. M. Hunter, and V. Sundström. 1994. Coherent nuclear motions and exciton-state dynamics in photosynthetic light-harvesting pigments. In *Ultrafast Phenomena IX*, Proceedings of the 9th International Conference, Dana Point, CA, May 2–6, 1994. P. F. Barbara, W. H. Knox, G. A. Mourou, and A. H. Zewail, editors. Springer-Verlag, Berlin. 435–436.
- DeVault, D. 1981. Quantum-Mechanical Tunnelling in Biological Systems. Cambridge University Press, Cambridge. 79–83.
- Eads, D. D., E. W. Castner, R. S. Alberte, L. Mets, and G. R. Fleming. 1989. Direct observation of energy transfer in a photosynthetic membrane: chlorophyll *b* to chlorophyll *a* energy transfer. *J. Phys. Chem.* 93:8271–8275.
- Gillbro, T., V. Sundström, A. Sandström, M. Spangfort, and B. Andersson. 1985. Energy transfer within the isolated light-harvesting chlorophyll *a/b* protein of photosystem II (LHC-II). *FEBS Lett.* 193:267–270.
- Gillie, J. K., G. J. Small, and J. H. Golbeck. 1989. Nonphotochemical hole-burning of the native antenna complex of photosystem I (PSI-200). *J. Phys. Chem.* 93:1620–1627.
- Gouterman, M. 1978. Optical spectra and electronic structure of porphyrins and related rings. In *The Porphyrins*, Vol. 3. D. Dolphin, editor. Academic Press, New York. 1–165.
- Hess, S., F. Feldshtein, A. Babin, I. Nurgaleev, T. Pullerits, A. Sergeev, and V. Sundström. 1993. Femtosecond energy transfer within the LH2 peripheral antenna of the photosynthetic purple bacteria *Rhodospirillum rubrum* and *Rhodospirillum rubrum* LL. *Chem. Phys. Lett.* 216:247–257.
- Houssier, C., and K. Sauer. 1970. Circular dichroism and magnetic circular dichroism of the chlorophyll and protochlorophyll pigments. *J. Am. Chem. Soc.* 92:779–791.
- Krawczyk, S., Z. Krupa, and W. Maksymiec. 1993. Stark spectra of chlorophylls and carotenoids in antenna pigment-proteins LHC-II and CP-II. *Biochim. Biophys. Acta.* 1143:273–281.
- Kwa, S. L. S., H. van Amerongen, S. Lin, J. P. Dekker, R. van Grondelle, and W. S. Struve. 1992. Ultrafast energy transfer in LHC-II trimers from the Chl *a/b* light-harvesting antenna of photosystem II. *Biochim. Biophys. Acta.* 1102:202–212.
- Manneback, C. 1951. Computation of the intensities of vibrational spectra of electronic bands in diatomic molecules. *Physica Grav.* 17:1001–1010.
- Savikhin, S., and W. S. Struve. 1994a. Femtosecond pump-probe spectroscopy of bacteriochlorophyll *a* monomers in solution. *Biophys. J.* 67:2002–2007.
- Savikhin, S., and W. S. Struve. 1994b. Ultrafast energy transfer in FMO trimers from the green bacterium *Chlorobium tepidum*. *Biochemistry.* 33:11200–11208.
- Savikhin, S., W. Zhou, R. E. Blankenship, and W. S. Struve. 1994. Femtosecond energy transfer and spectral equilibration in bacteriochlorophyll *a*—protein antenna trimers from the green bacterium *Chlorobium tepidum*. *Biophys. J.* 66:110–114.